



## Coupled fracture modes under anti-plane loading

Les P. Pook

21 Woodside Road, Sevenoaks TN13 3HF (UK)

les.pook@tesco.net

F. Berto

Department of Management and Engineering, University of Padova, Stradella S. Nicola 3, 36100, Vicenza (Italy)

berto@gem.unipd.it

A. Campagnolo

Department of Industrial Engineering, University of Padova, Via Venezia 1, 35131, Padova (Italy)

alberto.campagnolo@unipd.it

---

**ABSTRACT.** The linear elastic analysis of homogeneous, isotropic cracked bodies is a Twentieth Century development. It was recognised that the crack tip stress field is a singularity, but it was not until the introduction of the essentially two dimensional stress intensity factor concept in 1957 that widespread application to practical engineering problems became possible. The existence of three dimensional corner point effects in the vicinity of a corner point where a crack front intersects a free surface was investigated in the late 1970s: it was found that modes II and III cannot exist in isolation. The existence of one of these modes always induces the other. An approximate solution for corner point singularities by Bažant and Estensoro explained some features of corner point effects but there were various paradoxes and inconsistencies. In an attempt to explain these a study was carried out on the coupled in-plane fracture mode induced by a nominal anti-plane (mode III) loading applied to plates and discs weakened by a straight crack. The results derived from a large bulk of finite element models showed clearly that Bažant and Estensoro's analysis is incomplete. Some of the results of the study are summarised, together with some recent results for a disc under in-plane shear loading. On the basis of these results, and a mathematical argument, the results suggest that the stress field in the vicinity of a corner point is the sum of two singularities: one due to stress intensity factors and the other due to an as yet undetermined corner point singularity.

**KEYWORDS.** Finite elements; Mixed modes; Coupled modes; Stress intensity factors; Corner point singularities.

---

### INTRODUCTION

The linear elastic analysis of homogeneous, isotropic cracked bodies is a Twentieth Century development [1, 2], with the first papers appearing in 1907, but it was not until the introduction of the stress intensity factor concept in 1957 [3] that widespread application of linear elastic fracture mechanics (LEFM) to practical engineering

---



problems became possible. A stress intensity factor is the leading term of a series expansion of a crack tip stress field. The first application of finite elements to the calculation of stress intensity factors for two dimensional cases was in 1969 [4]. Finite element analysis had a significant influence on the development of LEFM. Corner point singularities were investigated in the late 1970s [5]. It was soon found that the existence of corner point effects made interpretation of calculated stress intensity factors calculated using finite element analysis difficult, and their validity questionable.

One of the main interests dealing with fracture mechanics is to quantify the crack tip surface displacement [6]. By superimposing the displacements due to the three modes of loading (mode I, mode II, mode III), shown in Fig. 1, it is possible to fully describe the crack tip surface displacements. If a crack surface is considered as consisting of points then the three modes of crack surface displacement provide an adequate description of the movements of crack surfaces when a load is applied. Assuming a Poisson's ratio,  $\nu$ , greater than zero, and also assuming that the crack front is perpendicular to a surface of a body, as is done in this paper, then it is possible to prove that modes II and III at the crack tip cannot exist in isolation [7, 8]. Mode II causes mode III<sup>c</sup> and mode III generates mode II<sup>c</sup>. These induced modes are properly named coupled modes. The superscript c is usually employed for their representation. There are no coupled modes when  $\nu$  is zero, and the magnitude of coupled modes increases with  $\nu$  [9]. It is not clear what happens when  $\nu$  is less than zero.

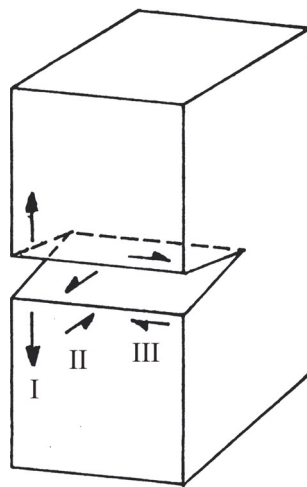


Figure 1: Notation for modes of crack tip surface displacement.

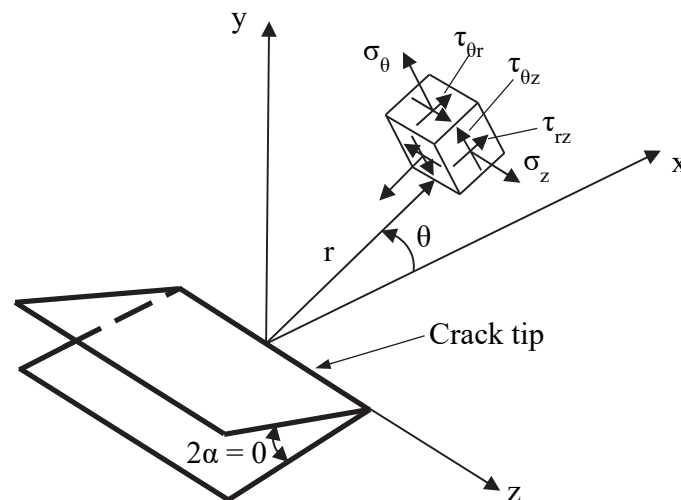


Figure 2: Notation for crack tip stress field.

A series expansion is able to represent the stress field in the neighbourhood of the crack tip [3, 10]. The leading order term of this series is the stress intensity factor,  $K$ . Subscripts I, II, II are used to denote mode. In agreement with the well known fracture mechanics framework, the stress components are proportional to  $K\sqrt{r}$  where  $r$  is the distance from the

crack tip (Fig. 2). Displacements are instead proportional to  $K\sqrt{r}$ . The leading order term tied to the stress intensity factor provides an accurate description of the stress field in a  $K$ -dominated region characterized by a radius  $r \approx a/10$  where  $a$  is crack length, [6].

The concept of a corner point singularity was introduced by Bažant and Estenssoro first and later by Pook [5, 11]. Some pioneering results were given also by Benthem [21]. An approximate solution showed that the of intensity of the stress field near the point of corner singularity can be done by defining a stress intensity measure called  $K_\lambda$ . However, explicit expressions for  $K_\lambda$ , and the stress and displacement fields associated to it are not available. The only statement based on the initial assumption used is that stresses are proportional to  $K_\lambda/r^\lambda$  and displacements to  $K_\lambda r^{1-\lambda}$ . The distance  $r$  is in this particular case the distance of a generic point from the corner point and  $\lambda$  is a function of Poisson's ratio.

Application of Bažant and Estenssoro's analysis was successful in explaining some aspects of behaviour in the vicinity of a corner point, but various paradoxes and inconsistencies appeared [1]. In an attempt to resolve these an extensive finite element research programme has been carried out [13-15]. The purpose of the present paper is to present some of the results obtained, and also to present a possible approach to resolution of paradoxes and inconsistencies.

### THE RESEARCH PROGRAMME

Two models were considered. Firstly, discs of finite thickness under anti-plane (remote nominal mode III) loading [13]. The radius of the disc,  $r$ , is equal to 50 mm. A through the thickness crack with its tip at the centre of the disc has been considered, with a length,  $a$ , equal to 50 mm. Different ratios have been considered between the disc thickness  $t$  and the crack length  $a$ . In particular the following ratios have been modelled:  $t/a = 0.25, 0.5, 0.75, 1, 1.25, 1.5, 1.75, 2, 2.25, 2.5, 2.75$  and 3. Finite element models have been analysed by means of ANSYS 11. Stress intensity factors were evaluated from the stress components in the neighbourhood of the crack tip using standard equations [6,10]. The material has been considered linear elastic and the Poisson's ratio has been set equal to 0.3 while the Young's modulus,  $E$ , has been set equal to 200 GPa. The load has been applied in terms of displacement on the nodes corresponding to the cylindrical surfaces. The applied displacements correspond to a nominal mode III stress intensity factor  $K_{III} = 1 \text{ MPa}\cdot\text{m}^{0.5}$  ( $31.62 \text{ N}\cdot\text{mm}^{0.5}$ ). Recently, results have been obtained for in-plane shear loading of a disc,  $t/a = 1$ . In plane displacements were applied on the cylindrical surface, corresponding to a nominal mode II stress intensity factor  $K_{II} = 1 \text{ MPa}\cdot\text{m}^{0.5}$  ( $31.62 \text{ N}\cdot\text{mm}^{0.5}$ ).

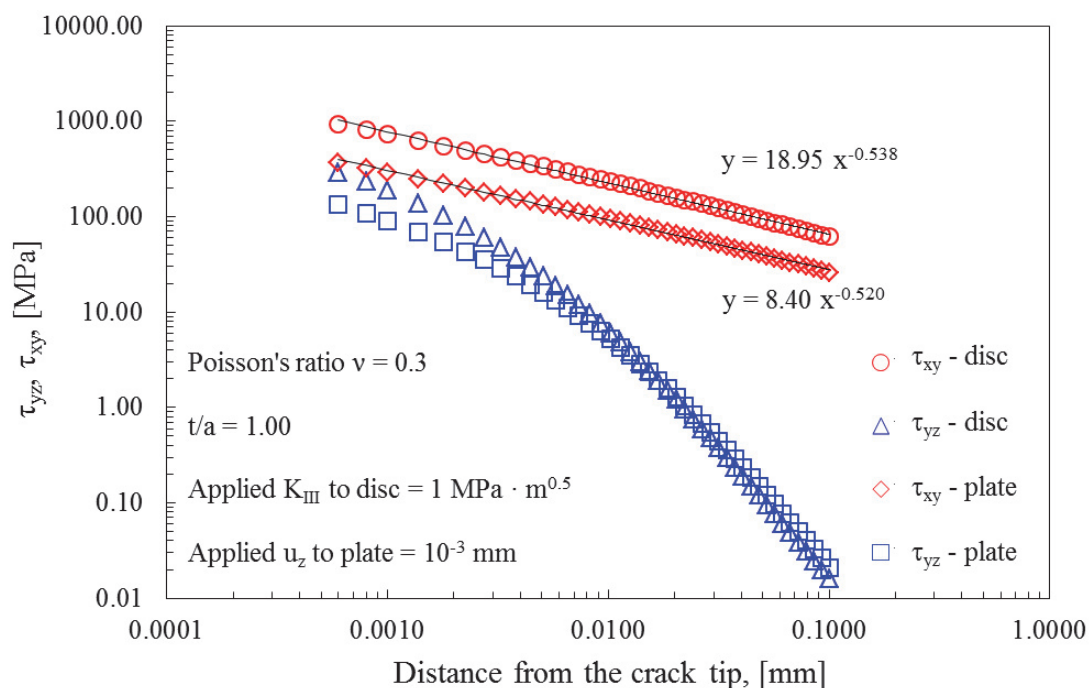


Figure 3: Stresses  $\tau_{yz}$  and  $\tau_{xy}$  on crack surface at  $s = 0$  mm from disc and plate surfaces,  $t/a = 1$ .



Secondly, plates of finite thickness under anti-plane (remote nominal mode III) [14]. A square plate with a constant width equal of 100 mm has been considered. The thickness of the plate  $t$  has been varied in the models keeping constant the crack length ( $a = 50\text{mm}$ ). The following ratios between  $t$  and  $a$  have been considered: 0.25, 0.5, 0.75, 1, 1.25, 1.5, 1.75, 2, 2.25, 2.5, 2.75 and 3. As for the case of the discs the material has been considered obeying a linear elastic law with  $\nu = 0.3$  and  $E = 200 \text{ GPa}$ . In this case the load has been applied by means of a constant displacement equal to  $10^{-3} \text{ mm}$  applied on the external edge of the plate. Displacements  $u_z$  were applied to the side containing the crack mouth.

$t/a$	$s = 0 \text{ mm}$		$s = 0.25 \text{ mm}$		$s = 1 \text{ mm}$	
	disc	plate	disc	plate	disc	plate
0.25	0.505	0.538	0.497	0.498	0.497 (0.508)	0.497 (0.507)
0.50	0.520	0.527	0.497	0.498	0.497 (0.506)	0.497 (0.506)
0.75	0.530	0.523	0.497	0.498	0.497 (0.507)	0.497 (0.506)
1.00	0.538	0.520	0.497	0.498	0.497 (0.507)	0.497 (0.506)
1.25	0.544	0.517	0.497	0.498	0.497 (0.506)	0.497 (0.506)
1.50	0.549	0.515	0.497	0.498	0.497 (0.506)	0.497 (0.506)
1.75	0.553	0.513	0.497	0.498	0.497 (0.506)	0.497 (0.506)
2.00	0.556	0.512	0.497	0.498	0.497 (0.506)	0.497 (0.506)
2.25	0.559	0.510	0.497	0.498	0.497 (0.507)	0.497 (0.506)
2.50	0.542	0.510	0.497	0.498	0.497 (0.506)	0.497 (0.505)
2.75	0.545	0.509	0.497	0.498	0.497 (0.506)	0.497 (0.506)
3.00	0.547	0.508	0.497	0.498	0.497 (0.507)	0.497 (0.506)

Table 1: Values of  $\lambda$  for  $\tau_{xy}$ ,  $s$  is the distance from the surface in the  $z$  direction. Values in brackets are for  $\tau_{yz}$ .

Stress components  $\tau_{yz}$  and  $\tau_{xy}$  were obtained from finite element models at different distances,  $s$ , from the free surfaces of the plate or disc. In particular, distances of 0 mm, 0.25 mm, 1 mm and 2 mm have been considered. Typical results are shown Fig. 3, plotted on logarithmic scales. Results from discs and plates are very similar. Values of  $\lambda$  obtained are listed in Tab. 1 comparing the results from discs and plates. For  $s = 0$  and 0.25 mm  $\tau_{yz}$  does not behave as a straight line. For values of  $s$  ranging between 0.25 to 2 mm the slope characterizing  $\tau_{xy}$  is constant and almost equal to the theoretical value of 0.5. Hence, Mode II stress intensity factor  $K_{II}$  can be correctly defined and calculated for these values of  $s$ . Dealing with cracked plates at  $s = 0$  the slope  $\lambda$  reaches its maximum at  $t/a = 0.25$  remaining in all the cases considered significantly lower than the value of 0.598 usually assumed for the case of a corner point singularity. These latest results are different from those obtained in the case of discs where the slope  $\lambda$  increases for increasing values of  $t/a$ . Both for plates and discs the mode III stress intensity factor  $K_{III}$  can be well defined at  $s = 1 \text{ mm}$  and  $2 \text{ mm}$  because the slope is close to that theoretically expected (0.5). For in plane shear loading stresses  $\tau_{yz}$  and  $\tau_{xy}$  on the crack surface at  $s = 0 \text{ mm}$  are similar to the stress distributions for nominal mode III loading. The value of  $\lambda$ , calculated from  $\tau_{xy}$ , is 0.541, is virtually the same as for nominal mode III loading.

The finite element results obtained at the coordinate  $s = 0$  (Fig. 4) show that the stress component  $\tau_{yz}$  is very far from the linear theoretical trend corresponding to a straight line on log log coordinates. This is true both for discs and plates, and the corresponding stress intensity factors are shown in Fig. 12: the apparent value of the mode III stress intensity factor  $K_{III}$  is strongly dependent on the coordinate  $x$ . For  $s=0$  realistic values of  $K_{III}$  cannot be calculated. Values of  $\lambda$ , calculated from  $\tau_{xy}$  and  $\tau_{yz}$ , are 0.499 and 0.506, in excellent agreement with the nominal mode III results. Similarly, stresses  $\tau_{yz}$  and  $\tau_{xy}$  on the crack surface at  $s = 2 \text{ mm}$  from the disc are similar to the stress distributions for nominal mode III loading. Values of  $\lambda$  are in excellent agreement. Distributions of  $K_{II}$  and  $K_{III}$  at  $s = 0 \text{ mm}$  from the disc surface are similar to those for nominal mode III loading, shown in Fig. 4. However, through the thickness distribution of  $K_{II}$  and  $K_{III}$ , differ from those for nominal mode III loading. This difference is because the use of nominal mode II loading has eliminated disc

bending. The results show that the change of loading mode from nominal mode III to nominal mode II has had no effect on the distributions of  $\tau_{yz}$  and  $\tau_{xy}$  on and near the crack surface, but has significantly changed the through thickness distributions of  $K_{II}$ ,  $K_{III}$ .

## DISCUSSION AND CONCLUSIONS

As previously pointed out [13-15] the results in Tab. 1 show that Bažant and Estenssoro's solution is incomplete. There is no clear pattern to values of  $\lambda$  shown in the table, and attempts to find a three dimensional stress function for the stresses in the vicinity of a corner point have so far been unsuccessful.

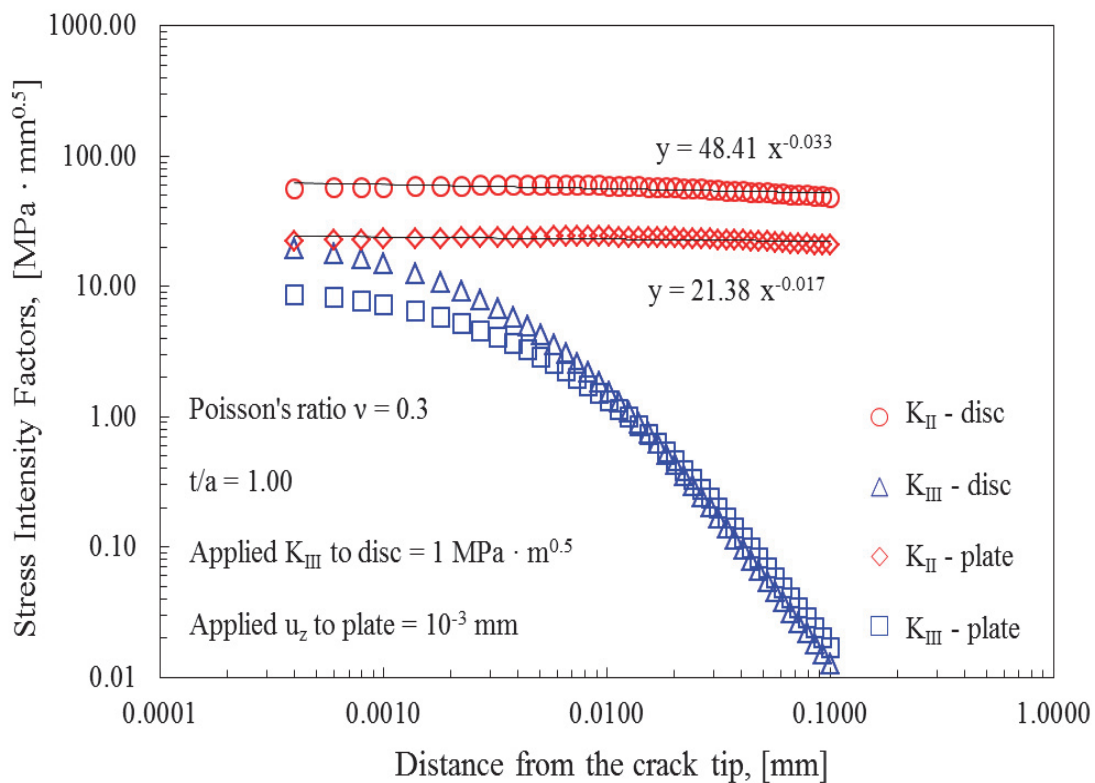


Figure 4:  $K_{II}$  and  $K_{III}$  at  $s = 0$  mm from disc and plate surfaces,  $t/a = 1$ .

A corner point stress function could be expected to reduce to a Westergaard stress function as a special case, but the following argument suggests that this is impossible. The Westergaard method of stress analysis [10] makes use of complex variables in which it is assumed that  $i^2 = -1$ . Complex numbers can be represented by a point on a plane. A three dimension equivalent to a Westergaard stress function would have to be based on a hypercomplex number system.

Hamilton's quaternions are a hypercomplex number system [16] that is sometimes used in elasticity [17]. In a quaternion it is assumed that  $i^2 = j^2 = k^2 = -1$ . A quaternion can be represented by a point in 4 dimensional space. Quaternions can be represented as pairs of complex numbers, but do not include complex numbers as a special case. A three dimensional equivalent of the Westergaard method would have to be based on quaternions. This suggests that a corner point stress function could not include Westergaard stress function as a special case.

This implies that stresses in the vicinity of a corner point are sums of stresses due to two different singularities of different orders: stress intensity factors and corner point singularities. The latter being asymptotic to zero as distance from the corner point increases. In other words Bažant and Estenssoro's analysis is incomplete. It is therefore not surprising that values of  $\lambda$  derived from finite element analysis are inconsistent.

To make progress the next step is to use the finite element results to separate the two singularities numerically and see whether this gives clues to the form of corner point singularities.



## REFERENCES

- [1] Pook, L.P., A 50-year retrospective review of three-dimensional effects at cracks and sharp notches. *Fatigue Fract. Engng. Mater. Struct.*, 36 (2013) 699-723.
- [2] Pook, L.P., The linear elastic analysis of cracked bodies and crack paths. *Theoretical and Applied Fracture Mechanics*, 79 (2015) 34-50.
- [3] Williams, M.L., On the stress distribution at the base of a stationary crack. *J. appl. Mech.*, 24 (1957) 109-114.
- [4] Dixon, J.R., Pook, L.P., Stress intensity factors calculated generally by the finite element technique. *Nature*, 224 (1969). 166-167.
- [5] Bažant, Z.P., Estenssoro, L.F., Surface singularity and crack propagation. *Int. J. Solids Struct.*, 15 (1979) 405-426.
- [6] Pook, L.P., *Linear elastic fracture mechanics for engineers. Theory and applications.* WIT Press, Southampton (2000)
- [7] Kotousov, A., Lazzarin, P., Berto, F., Pook, L.P. Three-dimensional stress states at crack tip induced by shear and anti-plane loading. *Eng. Fract. Mech.*, 108 (2013) 65-74.
- [8] Lazzarin, P., Zappalorto, M., A three-dimensional stress field solution for pointed and sharply radiused V-notches in plates of finite thickness. *Fatigue Fract. Eng. Mater. Struct.*, 35 (2012) 1105–1119.
- [9] Kotousov, A., Berto, F., Lazzarin, P., Pegorin, F., Three dimensional finite element mixed fracture mode under anti-plane loading of a crack. *Theoretical Appl. Fract. Mech.*, 62 (2012) 26-33.
- [10] Paris, P.C., Sih, G.C., *Stress analysis of cracks.* In *Fracture toughness testing and its applications.* ASTM STP 381. American Society for Testing and Materials, Philadelphia, (1965) 30-81.
- [11] Pook, L.P., Some implications of corner point singularities. *Eng. Fract. Mech.*, 48 (1994) 367-378.
- [12] Benthem, J.P., The quarter-infinite crack in a half-space; alternative and additional solutions. *Int. J. Solids Struct.*, 16 (1980) 119-130.
- [13] Pook, L.P., Berto, F., Campagnolo, A., Lazzarin, P., Coupled fracture mode of a cracked disc under anti-plane loading. *Eng. Fract. Mech.*, 128 (2014) 22-36.
- [14] Pook, L.P., Campagnolo, A., Berto, F., Lazzarin, P., Coupled fracture mode of a cracked plate under anti-plane loading. *Eng. Fract. Mech.*, 134 (2015) 391-403.
- [15] Pook, L.P., Campagnolo, A., Berto, F., Coupled fracture modes of discs and plates under anti-plane loading and a disc under in-plane shear loading. *Fatigue Fract. Eng. Mater. Struct.*, (2016) doi: 10.1111/ffe.12389
- [16] Pulver, S., Quaternions: the hypercomplex number system. *Mathematical Gazette*, 92 (2008) 431-436.
- [17] Weisz-Patrault, D., Bock, S., Gülebeck, K., Three-dimensional elasticity based on quaternion-valued potentials. *Int. J. Solids Struct.*, 51 (2014) 3422-3430.